Kelvin wave signatures in stratospheric trace constituents, Part II: water vapor

Philip W. Mote and Timothy J. Dunkerton

Northwest Research Associates, Bellevue, Washington

Hugh C. Pumphrey

Department of Meteorology, University of Edinburgh

———————

T.J. Dunkerton and P.W. Mote, Northwest Research Associates, PO Box 3027, Bellevue WA 98009. (mote@nwra.com, tim@nwra.com)

H.C. Pumphrey, Department of Meteorology, University of Edinburgh, King's Buildings, Mayfield Road, Edinburgh EH9 3JZ UK. (hcp@met.ed.ac.uk)

Abstract.   Kelvin waves are associated with variations in temperature
and winds in the tropical stratosphere on timescales of 5–20 days, and have
previously been linked to variations in several stratospheric trace constituents,
with the notable exception of water vapor. The present study examines wa-
ter vapor data from the Microwave Limb Sounder (MLS) to determine whether
variations on similar timescales are related to Kelvin waves. Some evidence
is found to link the variations in water vapor with Kelvin waves previously
identified in temperature, but the link is obscured by the sinuous background
profiles of water vapor induced by seasonal variations in saturation at the
tropical tropopause. Kelvin waves drive tropopause-level fluctuations in tem-
perature sufficiently large to cause substantial dehydration of air entering
the stratosphere.

1. Introduction

Stratospheric Kelvin waves have identifiable signatures in trace constituent fields [*Randel*, 1990; *Kawamoto et al.,* 1997]. In a companion paper, *Mote and Dunkerton* [200X] (hereinafter MD) described the signature of Kelvin waves in ozone, methane, nitrous oxide, and CFC-12, from two instruments aboard the Upper Atmosphere Research Satellite (UARS). This paper examines water vapor variations in the tropical stratosphere to determine whether Kelvin waves could be responsible for those variations.

Previous such efforts have had little or no success. *Randel* [1990] found Kelvin wave signatures in ozone (O_3) and nitric acid (HNO_3) in data from the Limb Infrared Monitor of the Stratosphere (LIMS), but found only weak and retrieval-dependent perturbations in water vapor (H_2O) and the signal was confined to the lower stratosphere. *Kawamoto et al.* [1997] also examined LIMS data for O_3 and H_2O, and, like Randel, found a weak signal of H_2O perturbations in the lower stratosphere. *Shiotani et al.* [1997] looked for Kelvin wave signatures in H_2O and O_3 observations from the Cryogenic Limb Array Etalon Spectrometer (CLAES), aboard the UARS, but reported that they "could not find significant signals" in these fields.

A better understanding of the influence of Kelvin waves on stratospheric water vapor, and especially on the tropical tropopause, would advance our understanding of key processes that determine water vapor. *Tsuda et al.* [1994], *Fujiwara et al.* [1998, 2001], and *Boehm and Verlinde* [2000] showed that Kelvin waves influence tropopause structure and upper tropospheric cirrus clouds, giving them an important role in stratosphere-troposphere exchange and the radiative properties of the upper troposphere. Indeed, the sharp cooling of the tropopause that is sometimes associated with Kelvin waves [e.g.,

Boehm and Verlinde, 2000] may be an important missing factor in the attempt to explain the observed water vapor mixing ratios in the stratosphere, which are generally thought to be lower than one would expect from considering time-mean tropical tropopause temperatures [e.g., *Zhou et al.*, 2001].

The rich vertical structure of water vapor poses special problems for the detection of Kelvin wave signatures in water vapor. The typical profile of tropical water vapor often includes at least three extrema as a result of the seasonal cycle of saturation mixing ratio at the tropical tropopause, which is then carried slowly upward in the tropical stratosphere – the "atmospheric tape recorder" [*Mote et al.*, 1996]. Unlike the earlier studies with LIMS and CLAES, we take this structure into account.

Mote et al. [1998] showed that MLS lower stratospheric water vapor (at 100 and 68 hPa) had spectral peaks at eastward wavenumber 1 at several periods between 6 and 20 days, suggestive of Kelvin wave activity. The challenge set forth in this paper is to determine whether water vapor variations in the stratosphere, and especially at 100 hPa where stratosphere-troposphere exchange might be detectable, can be linked with Kelvin waves.

2. Data

The Upper Atmosphere Research Satellite (UARS) [*Reber et al.,* 1993] was launched in September 1991. CLAES measurements ended when the cryogen ran out in early May 1993, and the MLS water vapor measurements ended with the failure of the 183 GHz radiometer in late April 1993. In MD can be found a brief description of the CLAES and Microwave Limb Sounder (MLS) instruments and their data products, notably tempera-

ture, which we use in this paper. Here we describe the MLS water vapor dataset, which was not presented by MD.

The most recent version of MLS data is Version 5 (V5) [*Livesey et al.*, 200X], which we use for temperature, but for water vapor we use an earlier version ("V0104") that is somewhat better in the lower stratosphere. Using the radiances from the 15 channels of band 5, centered on 183 GHz, V0104 uses a nonlinear retrieval for water vapor developed by *Pumphrey* [1999] that extends the sensitivity to 100 hPa. The V0104 data have been used in several previous studies of stratospheric water vapor [e.g., *Mote et al.,* 1998], and they clearly resolve the intricate vertical structure associated with seasonal variations in lower stratospheric water vapor, in agreement with the finer-resolution HALOE data [*Mote et al.,* 1996; *Pumphrey,* 1999]. Comparing V0104 data with balloon data, the mean difference is less than 0.1 ppmv in the lower stratosphere, and the rms difference is about 0.5 ppmv. V0104 data are systematically lower than HALOE data throughout the stratosphere, with a mean difference of about 0.2 ppmv in the lower stratosphere.

As in M02 and MD, we focus here on the time period July 1992–April 1993. *Mote et al.* [1998] examined both this time period and September 1991–May 1992, and found that the spectral characteristics of water vapor variations were similar in the two intervals. Hence we expect that repeating the analysis presented here for the earlier interval would produce substantially similar results.

3. Water vapor variations

Augmenting the Hovmöller (longitude-time) plots of water vapor at 100 and 68 hPa shown by *Mote et al.* [1998], we show in Figure 1 Hovmöller plots of variations in MLS temperature, CLAES temperature, and MLS water vapor at 46 hPa (the lowest level at

Figure 1

which all three data sets are available). The data have been highpass filtered to focus on timescales less than 30 days, and the zonal mean has been removed. Eastward-propagating features are common, especially in the CLAES data and especially in September 1992 and January–February 1993, as previously noted by *Mote et al.* [2002] and MD.

The coherence of features across the three plots is highlighted using multivariate extended empirical orthogonal functions (MEEOFs). MEEOFs, introduced by *Mote et al.* [2000], are a variation of EOFs that are useful for identifying space-time variations that are coherent among two or more fields. We use them here to produce longitude-lag basis vectors (Figure 1d–f) that capture leading modes of multi-field variance. As shown in Figure 1e, CLAES temperature variations have well-defined eastward-propagating maxima and minima, with period about 11 days. The zonal structure is predominantly wavenumber-one ($k = 1$), but $k = 2$ contributes as well, and the amplitude is largest just west of the dateline. MLS temperature variations are weaker (Figure 1a and 1d; see also MD, where the variance of MLS and CLAES temperature data were compared) and less coherent than CLAES, and appear to be somewhat out of phase with CLAES; this appears to be related to the lower sensitivity and vertical resolution of MLS (see MD).

Water vapor variations (Figure 1c and 1f) at this altitude share important characteristics with CLAES temperature variations, namely coherent eastward-propagating wavenumber-one features with period around 11–12 days. The zonal structure is almost purely $k = 1$, and without the $k = 2$ component, the phase speed is slower than for CLAES temperature. An important difference between the two temperature fields (Figure 1d, 1e) is that they are approximately out of phase; the reason for this will be explored in section 5.

Similar variations in MLS water vapor and CLAES temperature are found at all UARS

levels between 100 and 21 hPa (Figure 2). MEEOFs for just the two fields are calculated   Figure 2

at each level, and the structure and phase relationship between the two fields are different.

The dominant timescale at each level, as in Figure 1, is approximately 11–12 days. Water

vapor variations are very similar to temperature variations at 100 and 46 hPa (where

temperature leads by a quarter cycle), and bear some resemblance at 32 and 21 hPa

(where they are approximately in phase).

The characteristics of the variance in water vapor are rather different from those of

temperature. Following M02, we show power spectra for water vapor ($k = 1$) as functions

of altitude-frequency and latitude-frequency (Figure 3). For temperature (see M02, their   Figure 3

figure 2b) variance in the 4–30 day band was strongly concentrated between 7 and 10 days,

with a maximum in the upper stratosphere and large variance throughout the stratosphere.

As with temperature, water vapor variance is centered at the equator. Unlike temperature,

however, variance of water vapor is strongly concentrated in the lowest levels, especially

at 100 hPa, owing to occasional influence by the much wetter underlying troposphere.

Spectral power for water vapor is predominantly at lower frequencies than for temper-

ature. Very little power appears at the two dominant frequencies for temperature (9.6

days, indicated by the line, and 6 days). While one mode of temperature variations with

a period of around 17 days was identified by M02, it proved not to be a Kelvin wave, and

was small in the lower stratosphere. Variance at longer time scales (40–50 days) at 100

hPa is associated with the tropical intraseasonal oscillation, or Madden-Julian Oscillation

[*Mote et al.*, 2000]. The MEEOF analysis presented in Figure 2 highlighted a frequency

around 11 or 12 days. Apparently, the inclusion of water vapor in the variance matrix emphasizes somewhat slower variations than the dominant temperature variation.

Variations in water vapor and temperature are somewhat coherent for $k = 1$ (Figure 4), especially at longer periods (> 10 days) and at pressures roughly 20–40 hPa, and again in the upper stratosphere. The coherence is not as extensive as for ozone (see MD, their Figure 5) but still stand out above the noise level.

<div style="text-align: right">

Figure 4

</div>

4. Vertical connections

Despite the hints of coherence between stratospheric temperature and water vapor, the robust vertical connections of the variations throughout the stratosphere evident in temperature (M02) and in ozone, nitrous oxide, and to a lesser extent CF_2Cl_2 (MD) are not evident in water vapor. Time-height plots, EEOFs, and regression (not shown) reveal no obvious vertical connections, even though on any pressure surface the water vapor variations may closely resemble temperature variations, as in Figure 1. Vertical coherence of these variations only appears in the upper stratosphere from mid-December 1992 to the end of February 1993 (see Figure 6c), and perhaps from mid-December 1991 to mid-February 1992 (not shown). Otherwise, the variations show little obvious pattern. This section explores why there seems to be little connection between water vapor variations at different levels.

Kelvin waves are detectable in part because they cause vertical motions, displacing isopleths of temperature or trace constituents (q) that have nonzero vertical gradients:

$$(\frac{\partial}{\partial t} + u\frac{\partial}{\partial x})q' + w'q_z = 0 \tag{1}$$

On average, lower stratospheric water vapor is nearly constant between 100 and 10 hPa, but at any given time the vertical gradients q_z actually change sign — often two or three times. In fact, the vertical profile varies seasonally (Figure 5), owing to the upward propagation of the seasonally varying mixing ratio determined at the tropical tropopause [*Mote et al.*, 1996]. Consequently, the detection of Kelvin waves in lower stratospheric water vapor is considerably more challenging than their detection in temperature or monotonically changing trace constituents: the Kelvin wave signature in water vapor is confounded by the complex vertical structure that would result when the vertically coherent Kelvin signal (see Figure 5 of MD) is convolved with the seasonally varying water vapor profile.

4.1. Convolution of seasonal and intraseasonal variations

We explore the likely results of this convolution by constructing a putative Kelvin-wave water vapor field:

$$q'_T = T' \frac{\bar{q}_z}{\overline{T}_z} \tag{2}$$

where $\bar{q}_z$ is the (slowly varying) vertical gradient of zonal mean water vapor and $\overline{T}_z$ is the vertical gradient of zonal mean temperature. The field of Kelvin-wave temperature perturbations T' (Figure 6a) is constructed for each day using the first two EEOFs of MLS temperature (see M02 Figure 4) which together represent the 9.6-day Kelvin wave. (Note the shorter vertical extent of the temperature data: the EEOF analysis ended at 46 hPa, though regression analysis revealed a weak signal also at 68 hPa.)

The q'_T field (Figure 6b) is substantially different from T' owing to the influence of the "tape recorder" (which enters mathematically through multiplication by $\bar{q}_z$), which strongly damps the signal near zero lines and also appears to reverse the slope of the phase

lines at times, as in September 1992. Variations in q'_T are evident in August–September 1992 and faintly in January–February 1993, times when the Kelvin wave ampltitudes in temperature are large (MD, M02). The features in q'_T are quite shallow, often change sign in the vertical, and exhibit little coherence from level to level. Observed variations (Figure 6c) bear little resemblance to the q'_T, except perhaps from December 1992 to February 1993 in the upper stratosphere. Note the different ranges on the color bars in Figure 6b and Figure 6c.

When EEOFs of q'_T are calculated, the first six EEOFs are required merely to represent the Kelvin mode constructed from the first two EEOFs of temperature. With the variance spread among so many EEOFs, the eigenvalues are much smaller than those of the original temperature field. Little wonder, then, that when combined with other sources of variance (for example, other Kelvin modes, instrument noise), there is seldom any visible connection between water vapor variations observed at various levels (Figure 6c).

4.2. Does the retrieval limit detection of Kelvin wave signature in water vapor?

The vertical resolution of the MLS water vapor retrieval is approximately 3 km between 46 and 1 hPa [*Pumphrey,* 1999], or approximately one UARS level Δz, leading to some concern over whether the retrieval could successfully mimic the features shown in Figure 6b, some of which have vertical scale $2\Delta z$. To test the hypothesis that the retrieval sharply damps these variations, we used the q'_T data (Figure 6b) with random noise added at each level, along with the corresponding temperature variations, as input to the forward model described by *Pumphrey* [1999], which converts atmospheric profiles into radiances. The

resulting radiances were then fed into the retrieval code and "observed" profiles derived therefrom.

Results were high-pass filtered as in Figure 6b and are compared in Figure 7. The long-dashed line shows the linear best fit of the retrieved q_T' to the input q_T' for levels from 68 to 4.6 hPa (q_T' is constant at 100 hPa); the slope is 0.82, meaning that the mean reduction in amplitude by the forward model-retrieval combination is only 18%. Therefore, the retrieval appears to be capable of resolving features as sharp as those shown in Figure 6b, and we can apparently rule out the limitations of the retrieval as an explanation for the lack of coherent vertical structure in the water vapor.

$\boxed{\textbf{Figure 7}}$

5. Discussion and Conclusions

Variations in water vapor observed by MLS can be attributed to Kelvin waves, but their complex vertical structure prevents the easy identification that is possible for other trace constituents using simple statistical techniques (see MD). Although most variance in water vapor is at time scales longer than for temperature (Figure 3), significant variations occur at the timescales identified by M02 as dominating the temperature field, i.e., around 10 days and around 6 days. Based on the available evidence, it appears that these variations are indeed Kelvin waves. But our analysis has revealed no explanation for the apparent red-shifting of spectral power from temperature to water vapor.

In Figure 1, CLAES temperature and MLS water vapor appeared to be out of phase with each other, and MLS temperature was noisy but apparently not coherent with either of the other fields. The explanation for the lack of coherence between the two temperature fields was given by MD, and is probably related to the different vertical resolution of the two instruments, with MLS here at the bottom of its useful range and retrieving with

fairly coarse resolution. With the help of Figure 5, we can now understand why CLAES temperature and MLS water vapor might be out of phase: the MEEOFs are dominated by January–February 1993, when the vertical gradient of water vapor (though near zero) would tend to produce larger negative perturbations for downward displacements whereas for temperature downward displacements would produce positive perturbations.

Previous attempts to find Kelvin waves in satellite observations of water vapor [*Randel*, 1990 and *Kawamoto et al.,* 1997 with LIMS data; *Shiotani et al.,* 1997 with CLAES data] have failed, and it is now clear why. The previous studies attempted to find vertically coherent patterns without accounting for the "atmospheric tape recorder" which produces vertical structures in water vapor that are vastly different from those in temperature and other trace constituents. By focusing on individual levels, we have found Kelvin wave-like variations in much of the lower stratosphere.

The fact that the water vapor varies at Kelvin wave timescales at 100 hPa [Figure 3 and *Mote et al.,* 1998] suggests a possible role of Kelvin waves in stratosphere-troposphere exchange. Indeed, *Fujiwara et al.* [2001] noted that a Kelvin wave passing San Cristóbal Island in the eastern tropical Pacific produced stratosphere-troposphere exchange of ozone and water vapor, and the cooling produced by upward motion probably freeze-dried the air. Kelvin waves identified in ground-based data [*Fujiwara et al.,* 2001; *Holton et al.,* 2001] tend to have higher zonal wavenumber (2–4) and smaller vertical wavelength (3–7 km) than those identified in our satellite studies: M02 found waves with $k = 1$ and $k = 2$ whose vertical wavelength was 14–23 km, and MD noted that shorter wavelength waves would be strongly damped by the satellite retrievals.

Satellite observations of Kelvin waves have the obvious advantages of coverage that is more nearly global and continuous than the sporadic (but vertically detailed) station observations featured by *Fujiwara et al.* [2001] (two water vapor and three ozone soundings in September 1998) and *Holton et al.* [2001] (twice-daily temperature soundings for four weeks in June–July 1999). Unfortunately, with one exception, high-quality tropopause-level observations are not available from existing satellite measurements: MLS temperature is useless at 100 hPa, the retrieval of MLS water vapor at 100 hPa is actually dominated by variations at 68 hPa, MLS ozone data cannot be used below 46 hPa, CLAES ozone data are valid but poor at 100 hPa.

The exception is CLAES temperature, which is valid at least down to 146 hPa in the upper troposphere. We can combine the best feature of CLAES temperature (coverage into the troposphere) and the best feature of MLS temperature (far fewer gaps in time) by regressing the CLAES temperature onto the leading six principal components $\mathrm{PC}_i(t)$ of EEOF analysis of MLS temperature (see MD) to produce the spatial structure $\mathrm{T}_i(x, y, z)$, then forming the four-dimensional temperature $\mathrm{T}(x, y, z, t)$ as the sum over EEOFs

$$\mathrm{T}(x, y, z, t) = \Sigma_i \mathrm{PC}_i(t) \mathrm{T}_i(x, y, z).$$

The results are shown in Figure 8. On many occasions there is a clear connection from the stratopause down into the troposphere, with tropopause-level fluctuations as much as 8K (standard deviation 1.4K). Clearly, these Kelvin waves have the potential to influence global tropopause-level water vapor, but the magnitude of their influence cannot yet directly be evaluated.

Figure 8

References

Boehm, M.T., and J. Verlinde, Stratospheric influence on upper tropospheric tropical cirrus, *Geophys. Res. Lett., 27,* 3209–3212, 2000.

Fujiwara, M., K. Kita, and T. Ogawa, Stratosphere-troposphere exchange of ozone associated with the equatorial Kelvin wave as observed with ozonesondes and rawinsondes, *J. Geophys. Res., 103*, 19,173–19,182, 1998.

Fujiwara, M., F. Hasebe, M. Shiotani, N. Nishi, H. Vömel, and S.J. Oltmans, Water vapor control at the tropopause by the equatorial Kelvin wave observed over Galápagos, *Geophys. Res. Lett., 28*, 3143–3146, 2001.

Holton, J.R., M.J. alexander, and M.T. Boehm, Evidence for short vertical wavelength Kelvin waves in the Department of Energy-Atmospheric Radiation Measurement Nauru99 radiosonde data, *J. Geophys. Res., , 106,* 20,125–20,129, 2001.

Kawamoto, N., M. Shiotani, and J.C. Gille, Equatorial Kelvin waves and corresponding tracer oscillations in the lower stratosphere as seen in LIMS data. *J. Meteorol. Soc. Japan, 75,* 763–773, 1997.

Livesey, N.J., W.G. Read, L. Froidevaux, J.W. Waters, H.C. Pumphrey, D.L. Wu, M.L. Santee, Z. Shippony, R.F. Jarnot, The UARS Microwave Limb Sounder version 5 dataset: Theory, characterization and validation, *J. Geophys. Res.,* in press, 200X.

Mote, P.W., K.H. Rosenlof, M.E. McIntyre, E.S. Carr, J.C. Gille, J.R. Holton, J.S. Kinnersley, H.C. Pumphrey, J.M. Russell III, and J.W. Waters, An atmospheric tape recorder: The imprint of tropical tropopause temperatures on stratospheric water vapor. *J. Geophys. Res., 101,* 3989–4006, 1996.

Mote, P.W., T.J. Dunkerton, and H.C. Pumphrey, Sub-seasonal variations in lower strato-
spheric water vapor. *Geophys. Res. Lett., 25*, 2445–2448, 1998.

Mote, P.W., H.L. Clark, T.J. Dunkerton, R.S. Harwood, and H.C. Pumphrey, Intrasea-
sonal variations of water vapor in the tropical upper troposphere and tropopause region.
J. Geophys. Res., 105, 17,457–17,470, 2000.

Mote, P.W., T.J. Dunkerton, and D.L. Wu, Kelvin waves in stratospheric temperature ob-
served by the Microwave Limb Sounder, *J. Geophys. Res., 107*, 10.1029/2001JD001056,
2002.

Mote, P.W., and T.J. Dunkerton, Kelvin wave signatures in stratospheric trace con-
stituents, Part I. *J. Geophys. Res., ,* 200X.

Pumphrey, H.C., Validation of a new prototype water vapor retrieval for the UARS Mi-
crowave Limb Sounder. *J. Geophys. Res., 104*, 9399–9412, 1999.

Randel, W.J., Kelvin wave-induced trace constituent oscillations in the equatorial strato-
sphere. *J. Geophys. Res., 95*, 18,641–18,652, 1990.

Reber, C.A., C.E. Trevathan, R.J. McNeal, and M.R. Luther, The Upper ATmosphere
Research Satellite (UARS) Mission, *J. Geophys. Res., 98*, 10,643–10,647, 1993.

Shiotani, M., J.C. Gille, and A.E. Roche, Kelvin waves in the equatorial lower stratosphere
as revealed by cryogenic limb array etalon spectrometer temperature data, *J. Geophys.
Res., 102*, 26,131–26,140, 1997.

Tsuda, T., Y. Murayama, H. Wiryosumarto, S.W.B. Harijono, and S. Kato, Radiosonde
observations of equatorial atmospheric dynamics over Indonesia, 1. Equatorial waves
and diurnal tides, *J. Geophys. Res., 99,* 10,491–10,505, 1994.

Zhou, X.L., M.A. Geller, and M.H. Zhang, The cooling trend of the tropical cold point tropopause temperatures and its implications, *J. Geophys. Res.,* *106,* 1511–1522, 2001.

Figure 1.   Hovmöller (longitude-time) plots at 46 hPa of (a) temperature from MLS, (b) temperature from CLAES, and (c) water vapor from MLS. Gaps of longer than 2 days are indicated by hatched symbols. Contour interval for temperature 0.5K; for water vapor, 0.2 ppmv. In panels (d)–(f), the longitude-lag structure of the leading multivariate extended empirical orthogonal function (MEEOF) of the three fields is shown (see text for details). Units are dimensionless.

Figure 2.   Structure of variations in temperature (left column) and water vapor (right column) identified at each level using MEEOFs.

Figure 3.   Power spectra of MLS water vapor data for eastward wavenumber 1 shown (top) at the equator as a function of pressure and frequency and (bottom) at 68 hPa as a function of latitude and frequency. The long line in each panel shows the intersection point with the other panel. The short line indicates the period at which maximum power occurs in the temperature data (9.6 days; see *Mote et al.* [2002]).

Figure 4.   Coherence at the equator between CLAES temperature and MLS water vapor as a function of altitude and period.

Figure 5.   Mean tropical (7.5°S to 7.5°N) water vapor profiles for January–February 1993 (diamonds) and September 1992 (crosses). Note the repeated changes in the sign of the vertical gradient.

Figure 6.   Altitude-time plots along the equator of (a) temperature variations T' reconstructed using a Kelvin wave mode identified using empirical orthogonal function analysis; (b) water vapor variations derived from T' as described in the text; and (c) observed water vapor variations (cosine of wavenumber-one).

Figure 7.   Simulated water vapor as shown in Figure 6b and its retrieved value using the MLS retrieval. Solid diagonal line shows 1-1 correspondence, dashed line shows actual linear fit with slope 0.82 indicating average 18% loss of amplitude in retrieval. For greatest clarity, points in the central cluster ($q < 0.05$ ppmv) are shown using dots and points outside are shown using circles.

Figure 8.   CLAES temperature reconstructed using spatial structure derived by regressing CLAES temperature on MLS principal component time series (PC), then multiplying each PC by the corresponding structure and summing over the first six PCs. The time mean is then subtracted at each level. Contour interval 1.5K.

d   e   f
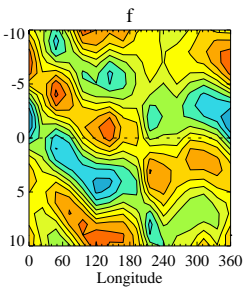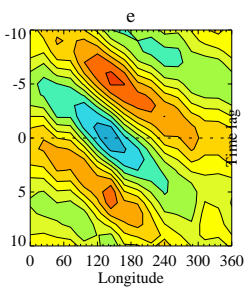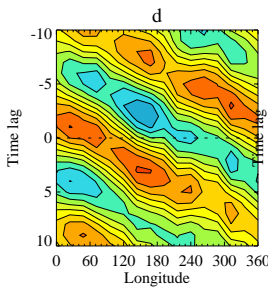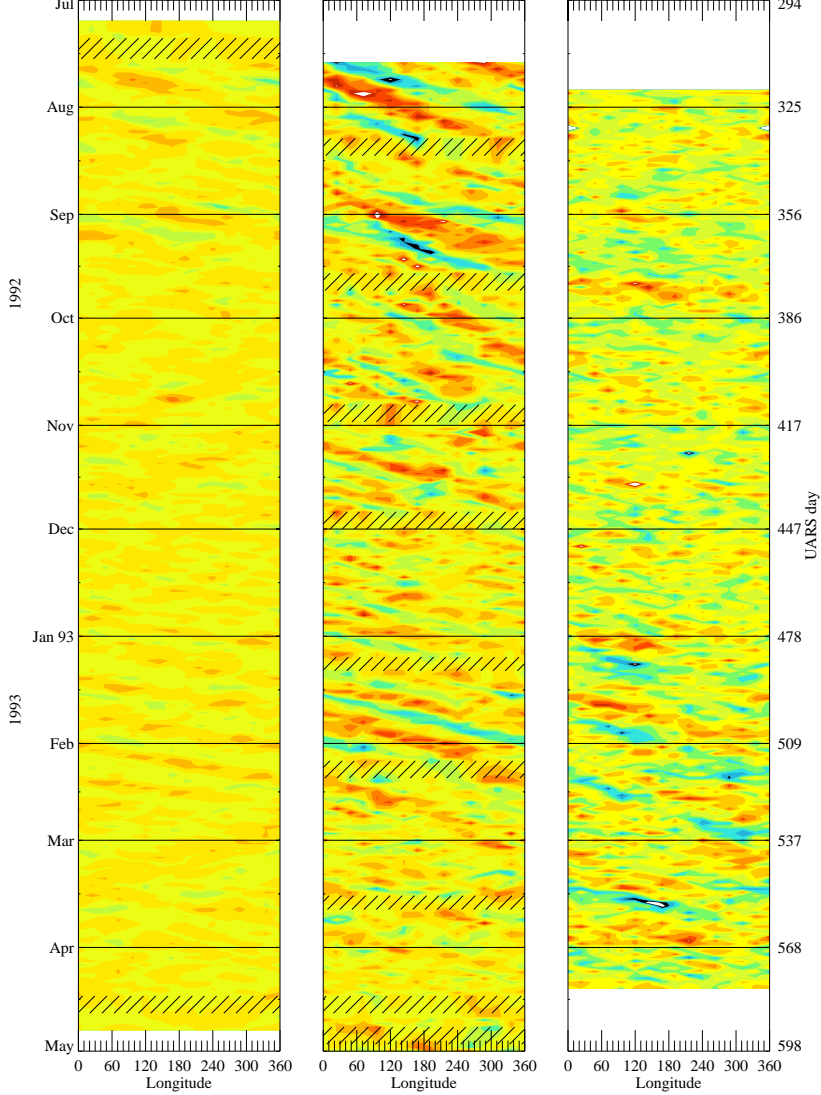
CLAES temperature at 21 hPa — MLS water vapor at 21 hPa
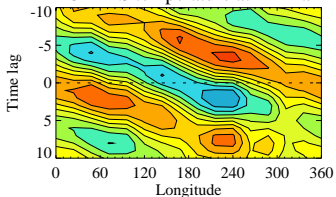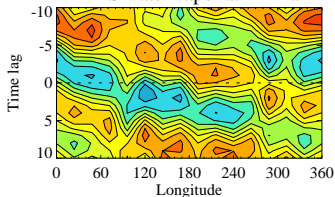
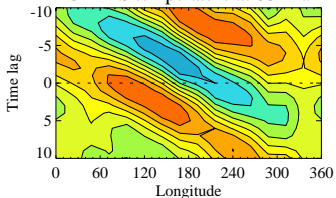CLAES temperature at 32 hPa — MLS water vapor at 32 hPa
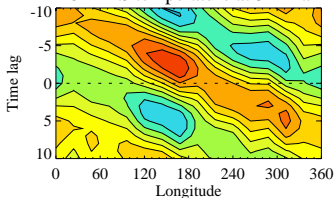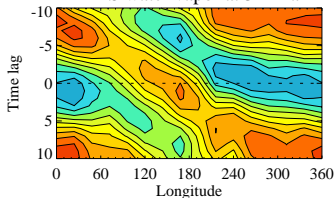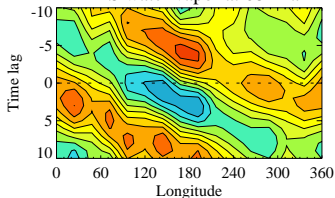
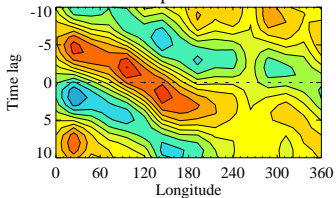CLAES temperature at 46 hPa — MLS water vapor at 46 hPa
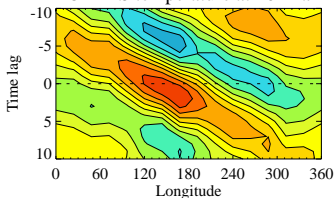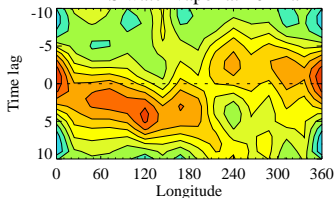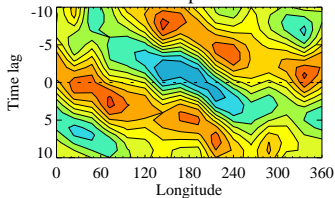
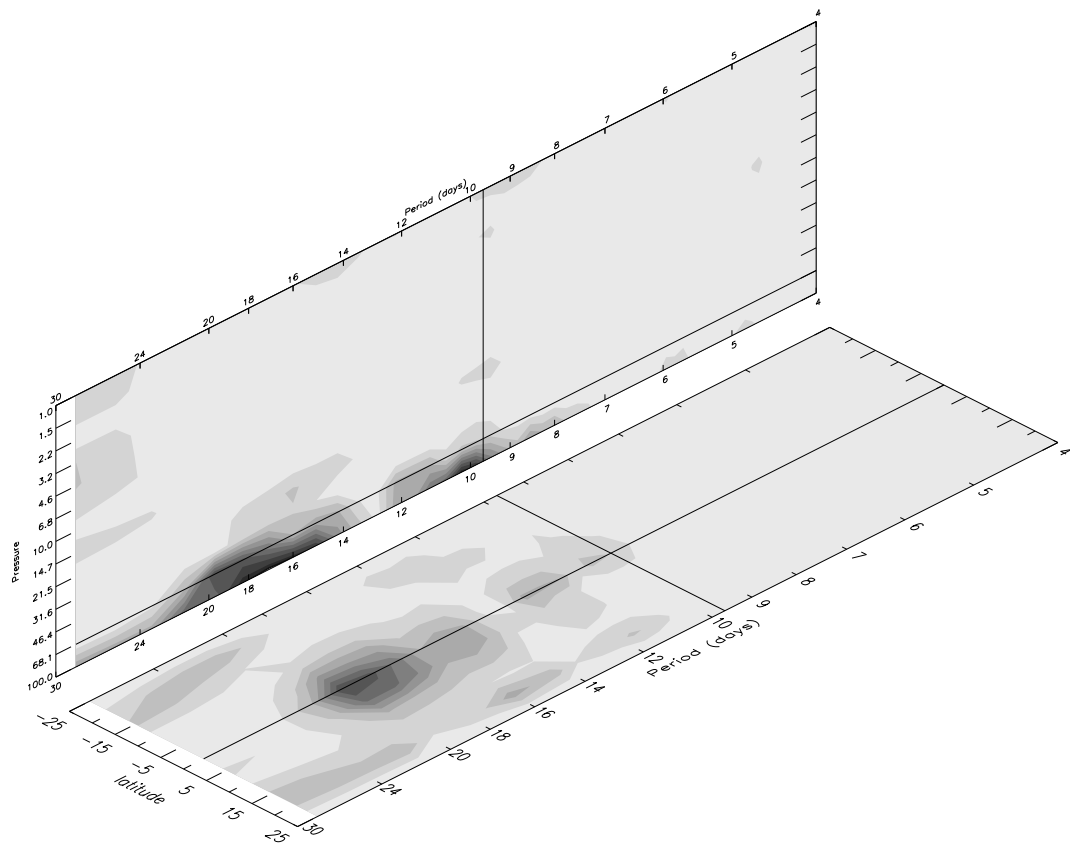CLAES temperature at 68 hPa — MLS water vapor at 68 hPa
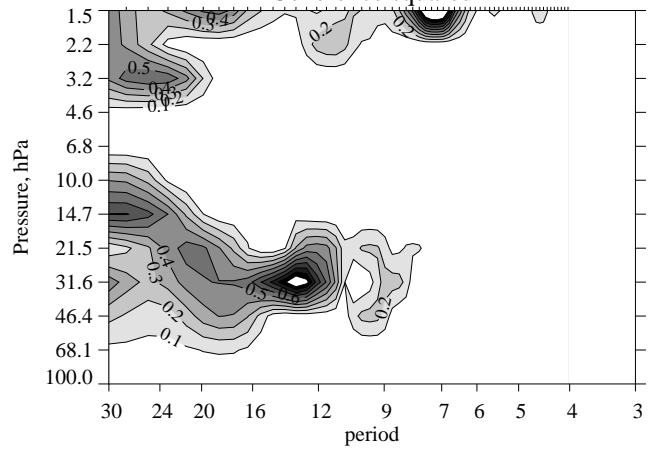
CLAES temperature at 100 hPa — MLS water vapor at 100 hPa

Coherence squared

Mean water vapor profiles

September 1992

Jan-Feb 1993

Pressure, hPa

ppmv

a. T′

b. q′$_T$

c. q′ obs